FRACTIONAL PENNES' BIOHEAT EQUATION: THEORETICAL AND NUMERICAL STUDIES

L.L. Ferrás [1,2], N.J. Ford [2], M.L. Morgado [3], J.M. Nóbrega [1], M. Rebelo [4]

Abstract

In this work we provide a new mathematical model for the Pennes' bioheat equation, assuming a fractional time derivative of single order. Alternative versions of the bioheat equation are studied and discussed, to take into account the temperature-dependent variability in the tissue perfusion, and both finite and infinite speed of heat propagation. The proposed bioheat model is solved numerically using an implicit finite difference scheme that we prove to be convergent and stable. The numerical method proposed can be applied to general reaction diffusion equations, with a variable diffusion coefficient. The results obtained with the single order fractional model, are compared with the original models that use classical derivatives.

MSC 2010: 35R11, 65N99, 92-08

Key Words and Phrases: Fractional differential equations, Caputo derivative, bioheat equation, stability, convergence.

1. Introduction

The way temperature diffuses in our body, has been a subject of interest for a long time. From the practical method of measuring the body temperature with our own hands, to the use of highly sophisticated measuring devices, we can find diverse alternative possibilities and intense theoretical and experimental research work that resulted in major advances and increased knowledge of temperature distribution inside the human body.

The pioneering work of Harry H. Pennes [33] in 1948 is the cornerstone of the mathematical modeling of temperature diffusion in tissues, but, as happens with most initial modelling approaches, it required some

pp. xxx–xxx, DOI: .....

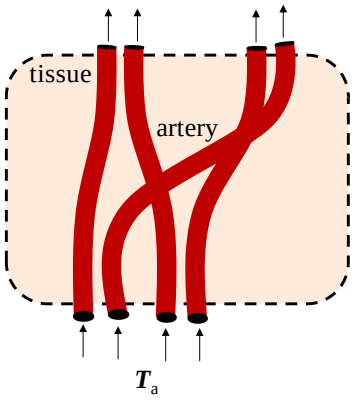

FIGURE 1. Heat transfer between blood vessels and tissue.

improvements. Moreover, this model was originally derived for modelling the temperature in a human forearm, but it is extensively used by several authors for modelling temperature diffusion in different tissues (such as the analysis of hyperthermia in cancer treatment [9]).

Pennes' [33] bioheat transfer equation (see also [30], [1], [36], [31], [24], [25]), which describes the thermal distribution in human tissue, taking into account the influence of blood flow, (see Fig. 1) is given by,

$$\rho_t c_t \frac{\partial T(x,t)}{\partial t} = k\frac{\partial^2 T(x,t)}{\partial x^2} + W_b c_b\,(T_a - T) + q_m, \quad t > 0,\ 0 < x < L, \tag{1.1}$$

where ρ_t, c_t are constants representing the density $\left[kg/m^3\right]$ and the specific heat $[J/\,(kg\,^\circ C)]$, respectively, and k is the tissue thermal conductivity$[J/(s.m\,^\circ C)]$; W_b is the mass flow rate of blood per unit volume of tissue $\left[kg/\left(s.m^3\right)\right]$; c_b is the blood specific heat; q_m is the metabolic heat generation per unit volume $\left[J/(s.m^3)\right]$; T_a represents the temperature of arterial blood $[^\circ C]$; T is the temperature and the term $W_b c_b\,(T_a - T)$ represents the blood perfusion. It is worth mentioning that the W_b constant was experimentally obtained by Pennes for a human forearm (he adjusted W_b until the temperature theoretical results matched the experimental ones).

In order to overcome Pennes' bioheat model limitations, other models have been proposed in the literature. Since in (1.1) the blood velocity field is not taken into account, in 1974, Wulff [41] and Klinger [23] considered the local blood mass flux to account for the blood flow direction. Also, Pennes assumed that thermal equilibration occurs in the capillaries, but in 1980 Chen and Holmes [5] showed that the major heat transfer processes occur in the 50 to 500 μm diameter vessels. Based on the Klinger model [23],

Chen and Holmes proposed a new model by adding dispersion and microcirculatory perfusion terms, and, in 1984, Weinbaum, Jiji and Lemons [39] presented a new vascular bioheat model by considering the countercurrent blood flow (this way, the blood leaving the tissue can also influence the temperature of the medium).

All these models, although sophisticated, do not take into account the role of thermoregulation. Therefore, in 2010, Zolfaghari and Maerefat [42] developed the simplified thermoregulatory bioheat (STB) model that takes into account the thermoregulatory mechanisms of the human body (shivering, regulatory sweating and vasomotion). The model is a combination of Pennes' bioheat equation and Gagge's two-node model (thermal comfort model) [13], [14]. This model proved to be reasonably accurate, showing a good fit to experimental data (for more on bioheat transfer see [27], [43]).

Although these models are more complete and, theoretically, more accurate than the classic Pennes' bioheat equation, their complexity makes them quite complicated to handle (some of the field variables, needed for the model to work, are difficult to obtain) and adjust to acquired experimental data. On the other hand, Pennes' equation is simple, with a small number of physical parameters, thus attracting researchers from different fields and encouraging the continued improvement of the model.

Different versions of this model have been proposed in the literature, that take into account the temperature-dependent variability in the tissue perfusion [24], [25], [8], [38], and, with the thermal conductivity being either depth-dependent or temperature-dependent.

The use of fractional calculus models for physical phenomena often leads to an improvement in the accuracy of the models (especially in processes with memory), and, Damor et al. [6] proposed a fractional version of the bioheat equation, by replacing the first-order time derivative with a derivative of arbitrary positive real order α (note that the equation written in this form is not dimensionally consistent, see Fig. 2),

$$\rho_t c_t \frac{\partial^\alpha T(x,t)}{\partial t^\alpha} = k \frac{\partial^2 T(x,t)}{\partial x^2} + W_b c_b \left(T_a - T\right) + q_m, \quad t > 0,\ 0 < x < L, \tag{1.2}$$

More recently, Ezzat et al. [10] (see also [20]) presented a new mathematical model for the Pennes' bioheat equation using a fractional version of the Fourier law for temperature. They constructed a model that comprises both the classic (parabolic) and hyperbolic Pennes' bioheat equation (note that the hyperbolic equation [32] ensures a finite speed pulse propagation while an infinite speed is obtained with the classic one), being given by,

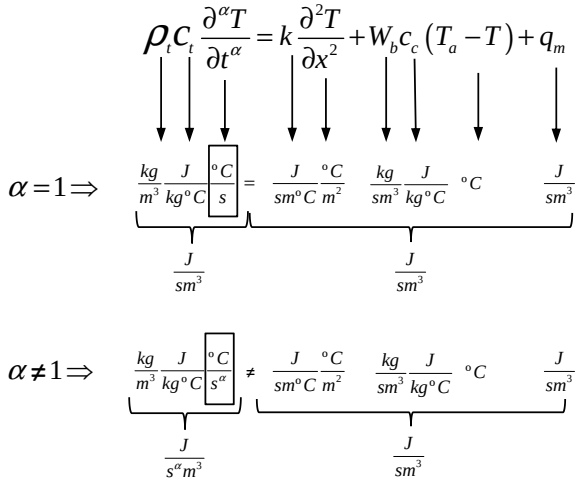

FIGURE 2. Dimensional analysis.

$$\rho_t c_t \frac{\partial}{\partial t}\left(T(x,t) + \frac{\tau^\alpha}{\alpha!}\frac{\partial^\alpha T(x,t)}{\partial t^\alpha}\right) = k\frac{\partial^2 T(x,t)}{\partial x^2} + \left(q_m(x,t) + \frac{\tau^\alpha}{\alpha!}\frac{\partial^\alpha q_m(x,t)}{\partial t^\alpha}\right), \quad t > 0,\ 0 < x < L. \tag{1.3}$$

Other versions of the model exist in the literature that basically are tailored versions of the original bioheat equation (1.1), with the purpose of modelling very specific cases.

In their paper [6], Damor et al. presented a method for the numerical solution of such equations. They do not provide any proof of convergence and stability of their method, and, they use a first order approximation for the discretisation of the Neumann boundary conditions. Another interesting work is the study proposed by Karatay et al. [22] where they present a new numerical scheme, based on the Crank-Nicholson method, for the solution of the time-fractional heat equation. In this work, we consider the fractional version of the Pennes's bioheat transfer equation (1.1), with the thermal diffusivity coefficient assumed as a function of space. In order to approximate the solution of this equation a numerical method is presented and the convergence and stability of the method are provided. Also, in our case the equation is dimensionally consistent.

The paper is organised as follows: in the next section we describe the fractional differential equation of single order used in this work; in Section **3** we describe the proposed numerical scheme, in Section **4** we prove the stability and convergence of the numerical scheme, in Section **5** we test the

convergence order of the method, and, perform numerical studies with the modified Pennes' model in Section 6. The paper ends with Section **7**, where we provide some conclusions and plans for further investigation.

2. Fractional bioheat equation

The bioheat equation presented before (1.1) is now adapted, using the time-fractional derivative instead of the first-order time derivative, $\frac{\partial T(x,t)}{\partial t}$, generalising in this way the original equation derived by Harry Pennes:

$$\frac{\partial^{\alpha} T(x,t)}{\partial t^{\alpha}} = A\frac{\partial}{\partial x}\left(k\left(x\right)\frac{\partial T(x,t)}{\partial x}\right) - BT(x,t) + C \quad 0 < t < T^{*},\ 0 < x < L, \tag{2.1}$$

where $\frac{\partial^{\alpha}}{\partial t^{\alpha}}$ is the fractional Caputo derivative of arbitrary real order α given by [7],

$$\frac{\partial^{\alpha} T(x,t)}{\partial t^{\alpha}} = \frac{1}{\Gamma\left(1-\alpha\right)}\int_{0}^{t}\left(t-s\right)^{-\alpha}\frac{\partial T(x,s)}{\partial s}ds \tag{2.2}$$

with $0 < \alpha < 1$, and $A = \frac{1}{\rho_t c_t \tau^{\alpha-1}}$, $B = \frac{W_b c_b}{\rho_t c_t \tau^{\alpha-1}}$, and $C = \frac{W_b c_b T_a + q_m}{\rho_t c_t \tau^{\alpha-1}}$. Note that $k\left(x\right)$ is a function of x, meaning that we can deal with possible anisotropy. Also, it is worth-mentioning the fact that we have added a new parameter $\tau\,[s]$ to the equation, so that it becomes dimensionally consistent. Alternatively, one could have assumed different coefficients from the ones used in the classical equation, and set the correct dimensions to these new parameters.

It should be noted that the fractional formulation has its origin in the generalisation of the Fourier law,

$$\mathbf{q} = -k\nabla T. \tag{2.3}$$

Gurtin and Pipkin [18] proposed a general non-local dependence in time, given by,

$$\mathbf{q} = -k\int_{0}^{\infty} K\left(u\right)\nabla T(t-u)\mathrm{d}u. \tag{2.4}$$

Assuming the substitution $\tau = t - u$ and choosing 0 as the starting point, we have the following equation,

$$\mathbf{q} = -k\int_{0}^{\infty} K\left(t-\tau\right)\nabla T(\tau)\mathrm{d}\tau, \tag{2.5}$$

that leads to the heat conduction equation with memory,

$$\frac{\partial T(x,t)}{\partial t} = a\int_{0}^{t} K\left(t-\tau\right)\triangle T(\tau)\mathrm{d}\tau. \tag{2.6}$$

If we assume that the nonlocal time dependence between the heat flux vector and the temperature gradient is given by the power kernel,

$$\mathbf{q} = -\frac{k_{pk}}{\Gamma(\alpha)} \frac{\partial}{\partial t} \int_0^{\infty} (t-\tau)^{\alpha-1} \nabla T(\tau) \mathrm{d}\tau, \;\; 0 < \alpha \leq 1, \tag{2.7}$$

then the corresponding heat equation is given by

$$\frac{\partial^{\alpha} T(x,t)}{\partial t^{\alpha}} = a \frac{\partial}{\partial x} \left(\frac{\partial T(x,t)}{\partial x} \right), \tag{2.8}$$

where a is the thermal diffusivity coefficient, with suitable dimensions [16], [34], [35].

If instead of the previous kernel we choose the "short-tail memory" with exponential kernel,

$$\mathbf{q} = -\frac{k_{stm}}{\xi} \int_0^{t} \exp\left(-\frac{t-\tau}{\xi} \right) \nabla T(\tau) \mathrm{d}\tau, \tag{2.9}$$

where ξ is a nonnegative constant, then the telegraph equation for temperature is obtained, [3], [4],

$$\frac{\partial T(x,t)}{\partial t} + \xi \frac{\partial}{\partial t} \left(\frac{\partial T(x,t)}{\partial t} \right) = a \frac{\partial}{\partial x} \left(\frac{\partial T(x,t)}{\partial x} \right). \tag{2.10}$$

Note that this telegraph equation solves the problem of infinite velocity propagation (a local perturbance in temperature is felt instantaneously in the entire medium), inherent to the classical temperature equation. The parameter ξ can be seen as thermal relaxation time, ranging from 10^{-8} to 10^{-14} $[s]$ in homogeneous substances, but, it may also take values of 30 $[s]$ in meat products [21].

In equation (2.1) we propose a new model, with a new parameter τ, but, an answer to the question "which values should be used for τ?" is a difficult task, since the physical meaning of τ is not yet defined.

Nonetheless, the fact that the time-fractional derivative promotes subdiffusion or superdiffusion, should not destroy or alter the well known properties of density and specific heat of the materials being studied (at least in a continuum approach). By looking at (2.7), we see that a new relationship between the heat flux and the temperature gradient is proposed, therefore, it can be assumed that instead of changing the density or specific heat, or creating a new model parameter, we are changing the thermal conductivity, k (see [26] for more information on anomalous heat conduction, and, the breakdown of the Fourier law). Taking as an example the equation proposed before for the anomalous diffusion, Eq. 2.8, this can be rewritten in the following way

$$\rho_t c_t \frac{\partial^\alpha T(x,t)}{\partial t^\alpha} = k_\alpha \frac{\partial}{\partial x}\left(\frac{\partial T(x,t)}{\partial x}\right) \tag{2.11}$$

where $k_\alpha = \frac{k_{pk}}{\tau^{\alpha-1}}$ is a "new" thermal conductivity. Generally speaking, if we keep the classical conservation of energy equation intact, then the time-fractional derivative will force changes in the relationship between the temperature flux and the temperature gradient, including the "anomalous" thermal conductivity coefficient.

2.1. Boundary conditions

We assume constant heat flux at the boundaries

$$-k(x)\left.\frac{\partial T(x,t)}{\partial x}\right|_{x=0} = q_0, \quad t > 0 \tag{2.12}$$

$$-k(x)\left.\frac{\partial T(x,t)}{\partial x}\right|_{x=L} = 0, \quad t > 0, \tag{2.13}$$

and an initial condition,

$$T(x,0) = T_a, \quad x \in (0,L). \tag{2.14}$$

This way we are assuming that at $x = 0$ we have a constant heat flux, and that "far" from that region, the zero temperature gradient applies. Besides the constant heat flux, we also consider periodic boundary conditions, given by,

$$-k(x)\left.\frac{\partial T(x,t)}{\partial x}\right|_{x=0} = q_0 cos\left(\omega t\right), \quad t > 0. \tag{2.15}$$

where ω is the heating frequency. It should be noted that one possible application of this type of boundary conditions is the tumor treatment by alternate cooling and heating [37].

3. Numerical solution

In order to obtain an approximate solution of Eq. (2.1), we need to approximate the time and spatial derivatives. For that, we consider a uniform space mesh on the interval $[0, L]$, defined by the gridpoints $x_i = i\Delta x$, $i = 0, \ldots, N$, where $\Delta x = \frac{L}{N}$, and we approximate the space derivative by the second order finite difference:

$$\begin{array}{l} \frac{\partial}{\partial x}\left(k\left(x\right)\frac{\partial T(x,t)}{\partial x}\right)\Big|_{x=x_i} = \\ \frac{k\left(x_i+\frac{\Delta x}{2}\right)T(x_{i+1},t)-\left(k\left(x_i+\frac{\Delta x}{2}\right)+k\left(x_i-\frac{\Delta x}{2}\right)\right)T(x_i,t)+k\left(x_i-\frac{\Delta x}{2}\right)T(x_{i-1},t)}{\left(\Delta x\right)^2} \\ +\mathcal{O}\left(\left(\Delta x\right)^2\right) \end{array} \tag{3.1}$$

For the discretisation of the fractional time derivative we also assume a uniform mesh, with a time step $\Delta t = T^*/R$ and time gridpoints $t_l = l\Delta t$, $l = 0,\, 1, ..., R$, and, we use the backward finite difference formula provided by Diethelm [7],

$$\begin{array}{rl} \frac{\partial^\alpha T(x,t)}{\partial t^\alpha} = & \frac{(\triangle t)^{-\alpha_j}}{\Gamma(2-\alpha_j)}\sum_{m=0}^{l} a_{m,l}^{(\alpha)}\left(T\left(x_i,t_{l-m}\right)-T\left(x_i,0\right)\right) \\ & +\mathcal{O}\left(\left(\Delta t\right)^{2-\alpha}\right) \end{array} \tag{3.2}$$

where

$$a_{m,l}^{(\alpha)} = \begin{cases} 1, & m=0, \\ \left(m+1\right)^{1-\alpha}-2m^{1-\alpha}+\left(m-1\right)^{1-\alpha}, & 0<m<l, \\ \left(1-\alpha\right)l^{-\alpha}-l^{1-\alpha}+\left(l-1\right)^{1-\alpha}, & m=l. \end{cases}$$

The coefficients $a_{m,l}^{(\alpha)}$ are such that

$$a_{m,l}^{(\alpha)} < 0, \quad m = 1,\, 2, ..., l-1 \tag{3.3}$$

$$\sum_{m=0}^{l} a_{m,l}^{(\alpha)} > 0, \;\; l = 1,\, 2, \ldots. \tag{3.4}$$

For a proof of these results see [11] and [28]. These properties will be useful when deriving the stability and convergence of the proposed method. Since the fractional derivate is a nonlocal operator, an increase in the computational effort is expected. To solve this problem, parallel algorithms can be used. The interested reader on the topic of parallel computing of fractional derivatives may consult the work by Gong et al. [15] where a parallel algorithm for the Riesz fractional reaction-diffusion equation is presented and explained.

Denoting the approximate value of $T\left(x_i,t_l\right)$ by T_i^l, and $k\left(x_i \pm \frac{\Delta x}{2}\right)$ by $k_{i\pm\frac{1}{2}}$ and neglecting the $\mathcal{O}\left(\left(\triangle x\right)^2\right)$ and $\mathcal{O}\left(\left(\triangle t\right)^{2-\alpha}\right)$ terms, the finite difference scheme is then given by,

$$\frac{(\triangle t)^{-\alpha}}{\Gamma(2-\alpha)}\sum_{m=0}^{l} a_{m,l}^{(\alpha)}\left(T_i^{l-m}-T_i^0\right) = A\frac{k_{i+\frac{1}{2}}T_{i+1}^l-\left(k_{i+\frac{1}{2}}+k_{i-\frac{1}{2}}\right)T_i^l+k_{i-\frac{1}{2}}T_{i-1}^l}{(\Delta x)^2} + f\left(x_i,t_l,T_i^l\right) \quad i=1,....,N-1,\ l=1,....,R, \tag{3.5}$$

with $f\left(x_i,t_l,T(x_i,t_l)\right)\sim f\left(x_i,t_l,T_i^l\right)=-BT_i^l+C$.

For consistency with the order of the spatial discretisation at grid points $i=2,....,N-2$, we also assume a second a order approximation for the Neumann boundary conditions. For that, a second order forward and backward finite difference formulae were used,

$$\left.\frac{\partial T(x,t_l)}{\partial x}\right|_{x=0} = \frac{-T(x_2,t_l)+4T(x_1,t_l)-3T(x_0,t_l)}{2\Delta x}+\mathcal{O}((\Delta x)^2), \tag{3.6}$$

$$\left.\frac{\partial T(x,t_l)}{\partial x}\right|_{x=L} = \frac{3T(x_N,t_l)-4T(x_{N-1},t_l)+T(x_{N-2},t_l)}{2\Delta x}+\mathcal{O}((\Delta x)^2) \tag{3.7}$$

This way we can obtain the following approximate expressions for the temperature at x_0 and x_N,

$$T_0^l \approx -\frac{1}{3}T_2^l+\frac{4}{3}T_1^l+\frac{2\Delta x f_0(t)}{3k(0)} \tag{3.8}$$

and

$$T_N^l \approx \frac{4}{3}T_{N-1}^l-\frac{1}{3}T_{N-2}^l-\frac{2\Delta x f_L(t)}{3k(L)} \tag{3.9}$$

where $f_0(t)$ stands for q_0 or $q_0 cos(\omega t)$ and $f_L(t)$ stands for 0. In order to keep the method as general as possible we will proceed using $f_0(t)$ and $f_L(t)$ (two functions of time) as the imposed fluxes.

We now present the system of equations that we need to solve. Using (3.8) and (3.9) in equations (3.5), for $i = 1$ and $i = N - 1$ we obtain:

$$\frac{(\triangle t)^{-\alpha}}{\Gamma(2-\alpha)} \sum_{m=0}^{l} a_{m,l}^{(\alpha)} \left(T_1^{l-m} - T_1^0 \right) = \left(k_{\frac{3}{2}} - \frac{1}{3} k_{\frac{1}{2}} \right) D T_2^l - \left(\left(k_{\frac{3}{2}} - \frac{1}{3} k_{\frac{1}{2}} \right) D + B \right) T_1^l + 2 k_{\frac{1}{2}} D \frac{f_0(t)\,\Delta x}{3 k_0} + C, \tag{3.10}$$

$$\frac{(\triangle t)^{-\alpha}}{\Gamma(2-\alpha)} \sum_{m=0}^{l} a_{m,l}^{(\alpha)} \left(T_{N-1}^{l-m} - T_{N-1}^0 \right) = - \left(\left(k_{\frac{2N-3}{2}} - \frac{1}{3} k_{\frac{2N-1}{2}} \right) D + B \right) T_{N-1}^l + \left(k_{\frac{2N-3}{2}} - \frac{1}{3} k_{\frac{2N-1}{2}} \right) D T_{N-2}^l - 2 k_{\frac{2N-1}{2}} D \frac{f_L(t_l)\,\Delta x}{3 k_N} + C. \tag{3.11}$$

For $i = 2, ..., N - 2$ we have:

$$\frac{(\triangle t)^{-\alpha}}{\Gamma(2-\alpha)} \sum_{m=0}^{l} a_{m,l}^{(\alpha)} \left(T_i^{l-m} - T_i^0 \right) = k_{i+\frac{1}{2}} D T_{i+1}^l - \left(\left(k_{i+\frac{1}{2}} + k_{i-\frac{1}{2}} \right) D + B \right) T_i^l + k_{i-\frac{1}{2}} D T_{i-1}^l + C \tag{3.12}$$

where $D = \dfrac{A}{(\Delta x)^2}$.

Introducing the vectors

$$\begin{aligned} \vec{x} &= \left[\begin{array}{cccc} x_1 & x_2 & \dots & x_{N-1} \end{array} \right]^{\mathrm{T}}, \\ \mathbf{T}^l &= \left[\begin{array}{cccc} T_1^l & T_2^l & \cdots & T_{N-1}^l \end{array} \right]^{\mathrm{T}}, \\ \frac{\partial^2 \mathbf{T}}{\partial x^2}(\vec{x}, t_l) &\left[\begin{array}{cccc} \frac{\partial^2 T}{\partial x^2}(x_1, t_l) & \frac{\partial^2 T}{\partial x^2}(x_2, t_l) \cdots & \frac{\partial^2 T}{\partial x^2}(x_{N-1}, t_l) \end{array} \right]^{\mathrm{T}}, \end{aligned} \tag{3.13}$$

the right-hand-side (rhs) of system of equations (3.10)-(3.12) can now be written in a discretised matrix form (for a time level l), as:

$$A \frac{\partial^2 \mathbf{T}}{\partial x^2}(\vec{x}, t_l) - B \mathbf{T}^l + C \approx \mathbf{M} \mathbf{T}^l + \mathbf{S}^l, \tag{3.14}$$

where

$$\mathbf{S}^l = \left[\begin{array}{ccccc} C + 2 k_{\frac{1}{2}} D \frac{\Delta x}{3 k(0)} f_0(t_l) & C & \cdots & C & C - 2 k_{\frac{2N-1}{2}} D \frac{\Delta x}{3 k_0} f_L(t_l) \end{array} \right]^{\mathrm{T}} \tag{3.15}$$

and

$$\mathbf{M}=\begin{bmatrix} \varphi_1(-1,-\frac{1}{3})D-B & \varphi_1(1,-\frac{1}{3})D & 0 & \dots & 0 & 0 \\ k_{\frac{5}{2}}D & -\varphi_2(1,1)D-B & k_{\frac{3}{2}}D & 0 & \dots & 0 \\ \dots & \ddots & \ddots & \ddots & \ddots & \dots \\ 0 & \ddots & k_{i+\frac{1}{2}}D & -\varphi_i(1,1)D-B & k_{i-\frac{1}{2}}D & \dots \\ 0 & \dots & \dots & 0 & \varphi_{N-1}(-\frac{1}{3},1)D & \varphi_{N-1}(\frac{1}{3},-1)D-B \end{bmatrix}, \tag{3.16}$$

with $\varphi_i(w_1,w_2)=w_1k_{i+\frac{1}{2}}+w_2k_{i-\frac{1}{2}}$.

The approximation (3.2), at $(x,t)=(x_i,t_l)$, for the time fractional derivative can be written as,

$$\frac{\partial^\alpha T}{\partial t^\alpha}(x_i,t_l)\approx\frac{(\triangle t)^{-\alpha}}{\Gamma(2-\alpha)}\left(T_i^l+\sum_{m=1}^{l-1}a_{m,l}^{(\alpha)}\left(T_i^{l-m}\right)-\sum_{m=1}^{l-1}a_{m,l}^{(\alpha)}T_i^0-T_i^0\right), \tag{3.17}$$

or, in matrix form,

$$\frac{\partial^\alpha \mathbf{T}}{\partial t^\alpha}(\vec{x},t_l)\approx\frac{(\triangle t)^{-\alpha}}{\Gamma(2-\alpha)}\left(\mathbf{T}^l+\sum_{m=1}^{l-1}a_{m,l}^{(\alpha)}\mathbf{T}^{l-m}-\sum_{m=1}^{l-1}a_{m,l}^{(\alpha)}\mathbf{T}^0-\mathbf{T}^0\right). \tag{3.18}$$

From the previous considerations we are now in position to describe the numerical scheme. Assume that we are at time level l and that we know the temperature field from the previous time levels, then from (3.14) and (3.18) the system of equations that needs to be solved can be written as

$$\mathbf{T}^l+\sum_{m=1}^{l-1}\left[a_{m,l}^{(\alpha)}\mathbf{T}^{l-m}\right]-\mathbf{T}^0\sum_{m=1}^{l-1}a_{m,l}^{(\alpha)}-\mathbf{T}^0=\Lambda\mathbf{M}\mathbf{T}^l+\Lambda\mathbf{S}^l \tag{3.19}$$

with $\Lambda=\dfrac{\Gamma(2-\alpha)}{(\triangle t)^{-\alpha}}$. Or, in an equivalent form,

$$(\mathbf{I}-\Lambda\mathbf{M})\,\mathbf{T}^l=-\sum_{m=1}^{l-1}\left[a_{m,l}^{(\alpha)}\mathbf{T}^{l-m}\right]+\mathbf{T}^0+\mathbf{T}^0\sum_{m=1}^{l-1}a_{m,l}^{(\alpha)}+\Lambda\mathbf{S}^l \tag{3.20}$$

The matrix $\mathbf{I}-\Lambda\mathbf{M}$, where $\mathbf{I}$ is the $(N-1)\times(N-1)$ identity matrix, is a strictly diagonally dominant matrix. Therefore the matrix $\mathbf{I}-\Lambda\mathbf{M}$ is invertible and the system (3.20) admits a unique solution given by

$$\mathbf{T}^l = (\mathbf{I} - \Lambda\mathbf{M})^{-1} \left(-\sum_{m=1}^{l-1} \left[a_{m,l}^{(\alpha)} \mathbf{T}^{l-m} \right] + \mathbf{T}^0 + \mathbf{T}^0 \sum_{m=1}^{l-1} a_{m,l}^{(\alpha)} + \Lambda \mathbf{S}^l \right) \quad (3.21)$$

4. Stability and convergence of the difference scheme

In this section we will prove the stability and convergence of the proposed method. Some of the ideas used in the demontrations were based on the excelent work by Huang et al. [19].

4.1. Stability of the difference scheme

For the proof of stability, the following lemma will be used.

LEMMA **4.1**. *Let* $\mathbf{L}$ *be an arbitrary square matrix. Then for any* $\varepsilon > 0$ *there exists a norm, denoted by* $\|.\|_\varepsilon$*, such that* $\|\mathbf{L}\|_\varepsilon \leq \rho(\mathbf{L}) + \varepsilon$.

THEOREM **4.1**. *Let* $0 < \varepsilon \leq \Delta t$*, the scheme given by (*3.21*) is unconditionally stable with respect to the initial conditions.*

P r o o f. For the proof of this result, we will assume the existence of two different vector solutions, $\mathbf{H}_1^l$ and $\mathbf{H}_2^l$ (that satisfy Eq. 3.21) with different initial conditions $\left(\mathbf{H}_1^0 \neq \mathbf{H}_2^0\right)$ but same boundary conditions. The difference $\mathbf{H}^l = \mathbf{H}_1^l - \mathbf{H}_2^l$ satisfies the following equation,

$$(\mathbf{I} - \Lambda\mathbf{M})\,\mathbf{H}^l = -\sum_{m=1}^{l-1} \left[a_{m,l}^{(\alpha)} \mathbf{H}^{l-m} \right] + \mathbf{H}^0 + \mathbf{H}^0 \sum_{m=1}^{l-1} a_{m,l}^{(\alpha)} \quad (4.1)$$

From Lemma **4.1** we know that, given $\varepsilon > 0$, there exists a norm $\|.\|_\varepsilon$ such that

$$\left\| (\mathbf{I} - \Lambda\mathbf{M})^{-1} \right\|_\varepsilon \leq \rho\left((\mathbf{I} - \Lambda\mathbf{M})^{-1} \right) + \varepsilon. \quad (4.2)$$

Using (4.2), for $l = 1$ we obtain

$$\begin{aligned} \left\| \mathbf{H}^1 \right\|_\varepsilon = \left\| (\mathbf{I} - \Lambda\mathbf{M})^{-1} \mathbf{H}^0 \right\|_\varepsilon &\leq \left\| (\mathbf{I} - \Lambda\mathbf{M})^{-1} \right\|_\varepsilon \left\| \mathbf{H}^0 \right\|_\varepsilon \\ &\leq \left(\rho\left((\mathbf{I} - \Lambda\mathbf{M})^{-1} \right) + \varepsilon \right) \left\| \mathbf{H}^0 \right\|_\varepsilon \quad (4.3) \end{aligned}$$

Since Λ, D, B and k_i are all positive, using the Gerschgorin Theorem is straightforward to prove that $\rho(\mathbf{I} - \Lambda\mathbf{M}) > 1$ which implies

$$\rho\left((\mathbf{I} - \Lambda\mathbf{M})^{-1} \right) < 1. \quad (4.4)$$

Hence, from (4.3) it follows

$$\left\|\mathbf{H}^1\right\|_\varepsilon \leq (1+\varepsilon)\left\|\mathbf{H}^0\right\|_\varepsilon . \tag{4.5}$$

Now, assume that the following relationship holds,

$$\left\|\mathbf{H}^k\right\|_\varepsilon \leq (1+\varepsilon)^k \left\|\mathbf{H}^0\right\|_\varepsilon \; k=1,2,...,l \tag{4.6}$$

we will prove $\left\|\mathbf{H}^{l+1}\right\|_\varepsilon \leq (1+\varepsilon)^{l+1}\left\|\mathbf{H}^0\right\|_\varepsilon$.

From (3.3), (3.4), (4.4) and (4.6), it can be deduced that

$$\begin{aligned}
\left\|\mathbf{H}^{l+1}\right\|_\varepsilon &\leq \left\|(\mathbf{I}-\Lambda\mathbf{M})^{-1}\right\|_\varepsilon \left\|\sum_{m=1}^{l}\left[\left(-a_{m,l+1}^{(\alpha)}\right)\mathbf{H}^{l+1-m}\right]+\mathbf{H}^0+\mathbf{H}^0\sum_{m=1}^{l}\left(a_{m,l+1}^{(\alpha)}\right)\right\|_\varepsilon \\
&\leq (1+\varepsilon)\left(\left\|\sum_{m=1}^{l}\left[\left(-a_{m,l+1}^{(\alpha)}\right)\mathbf{H}^{l+1-m}\right]\right\|_\varepsilon+\left[1+\sum_{m=1}^{l}\left(a_{m,l+1}^{(\alpha)}\right)\right]\left\|\mathbf{H}^0\right\|_\varepsilon\right) \\
&\leq (1+\varepsilon)\left(\left[\sum_{m=1}^{l}(-a_{m,l+1}^{(\alpha)})\right](1+\varepsilon)^j\left\|\mathbf{H}^0\right\|_\varepsilon+\left[1+\sum_{m=1}^{l}(a_{m,l+1}^{(\alpha)})\right](1+\varepsilon)^l\left\|\mathbf{H}^0\right\|_\varepsilon\right) \\
&\leq (1+\varepsilon)^{l+1}\left\|\mathbf{H}^0\right\|_\varepsilon \leq e^{(l+1)\varepsilon}\left\|\mathbf{H}^0\right\|_\varepsilon
\end{aligned} \tag{4.7}$$

Assuming $0<\varepsilon\leq\Delta t$, from (4.7) it follows that

$$\left\|\mathbf{H}^{l+1}\right\|_\varepsilon \leq e^{T^*}\left\|\mathbf{H}^0\right\|_\varepsilon ,$$

meaning that our numerical scheme is unconditionally stable with respect to the initial conditions.

□

4.2. Convergence analysis

Let us define the vector of the errors at time step l:

$$\mathbf{e}^l=\left[e_1^l,\, e_2^l,...,e_{N-1}^l\right], \quad l=1,2,...,$$

where $e_i^l=T(x_i,t_l)-T_i^l$ $l=1,2,...,$ $i=1,...,N-1$ is the error at each point of the mesh.

Let $\mathbf{T}_{an}^l=\left[\begin{array}{ccccc} T(x_1,t_l) & T(x_2,t_l) & \cdots & T(x_{N-2},t_l) & T(x_{N-1},t_l)\end{array}\right]^{\mathrm{T}}$ be the vector containing the exact solution for each node i (at time step l).

It can be easily seen that $\mathbf{T}_{an}^l$ satisfies the following equation,

$$\begin{aligned}
(\mathbf{I}-\Lambda\mathbf{M})\,\mathbf{T}_{an}^l = \; & -\sum_{m=1}^{l-1}\left[a_{m,l}^{(\alpha)}\mathbf{T}_{an}^{l-m}\right]+\mathbf{T}_{an}^0+\mathbf{T}_{an}^0\sum_{m=1}^{l-1}a_{m,l}^{(\alpha)} \\
& +\Lambda\mathbf{S}^l+\boldsymbol{\Lambda}\mathbf{R}^l
\end{aligned} \tag{4.8}$$

where $\mathbf{R}^l=[R_1^l,\quad R_2^l,.....,R_{N-1}^l]$ is a $(N-1)\times 1$ vector containing the errors committed in the discretisation of the derivative operators. If $T(x,t)$ is sufficiently regular, from (3.1), (3.2), (3.6) and (3.7) it is straightforward

prove that the truncation error at each point (x_i, t_l), $i = 1, \ldots, N-1$ satisfies

$$R_i^l = \mathcal{O}\left((\Delta x)^2\right) + \mathcal{O}\left((\triangle t)^{2-\alpha}\right). \tag{4.9}$$

On the other hand, the approximate solution $\mathbf{T}^l$ obtained from the proposed method satisfies

$$(\mathbf{I} - \Lambda\mathbf{M})\,\mathbf{T}^l = -\sum_{m=1}^{l-1}\left[a_{m,l}^{(\alpha)}\mathbf{T}^{l-m}\right] + \mathbf{T}^0 + \mathbf{T}^0\sum_{m=1}^{l-1} a_{m,l}^{(\alpha)} + \Lambda\mathbf{S}^l. \tag{4.10}$$

Subtracting (4.10) from (4.8) we have (notice that $\mathbf{e}^0 = [0,\, 0, ..., 0]$),

$$\mathbf{e}^l = (\mathbf{I} - \Lambda\mathbf{M})^{-1}\left(\sum_{m=1}^{l-1}\left[\left(-a_{m,l}^{(\alpha)}\right)\mathbf{e}^{l-m}\right] + \mathbf{\Lambda}\mathbf{R}^l\right) \tag{4.11}$$

Therefore, for $l = 1, 2, \ldots, R$ we have

$$\begin{aligned}\left\|\mathbf{e}^l\right\|_\varepsilon &\leq (1+\varepsilon)\left\|\sum_{m=1}^{l-1}\left[\left(-a_{m,l}^{(\alpha)}\right)\mathbf{e}^{l-m}\right]\right\|_\varepsilon + \Lambda\,(1+\varepsilon)\left\|\mathbf{R}^l\right\|_\varepsilon \\ &\leq (1+\varepsilon)\sum_{m=1}^{l-1}\left(-a_{m,l}^{(\alpha)}\right)\left\|\mathbf{e}^{l-m}\right\|_\varepsilon + \Lambda\,(1+\varepsilon)\left\|\mathbf{R}^l\right\|_\varepsilon, \end{aligned} \tag{4.12}$$

where ϵ is a positive constant such that $\varepsilon < \Delta t$.

Let us define a sequence $\{p_l\}_{l\in\mathbb{N}_0}$ such that $p_l - p_{l+1} = a_{m,l+1}^{(\alpha)}$, $m = 0, 1, \ldots, l-1$. Then $p_l = (l+1)^{1-\alpha} - l^{1-\alpha}$, $l = 0, 1, \ldots$, and from (3.3) we can conclude that p_l is a decreasing sequence. Taking this into account, in what follows we prove by induction on l, that

$$\left\|\mathbf{e}^l\right\|_\varepsilon \leq C\Lambda\,(1+\varepsilon)^l\,p_{l-1}^{-1}\left((\Delta t)^{2-\alpha} + (\Delta x)^2\right), \quad l = 0, 1, \ldots \tag{4.13}$$

From (4.12) and (4.9) we obtain

$$\left\|\mathbf{e}^1\right\|_\varepsilon \leq \Lambda\,(1+\varepsilon)\left\|\mathbf{R}^1\right\|_\varepsilon \leq C\Lambda\,(1+\varepsilon)\,p_0^{-1}\left((\Delta t)^{2-\alpha} + (\Delta x)^2\right), \tag{4.14}$$

then (4.13) is valid for $l = 1$. Now, suppose we have

$$\left\|\mathbf{e}^j\right\|_\varepsilon \leq C\,\Lambda\,(1+\varepsilon)\;p_{j-1}^{-1}\left((\Delta t)^{2-\alpha} + (\Delta x)^2\right), \quad j = 1, 2, \ldots, l \tag{4.15}$$

we want to prove that

$$\left\|\mathbf{e}^{l+1}\right\|_\varepsilon \leq C\,\Lambda\,(1+\varepsilon)\;p_l^{-1}\left((\Delta t)^{2-\alpha} + (\Delta x)^2)\right)\,. \tag{4.16}$$

From (4.12), (4.9), (4.15), and using some properties of the sequences p_l and $a_{m,j}^{(\alpha)}$ (explained before), we obtain

$$\begin{aligned}\left\|\mathbf{e}^{l+1}\right\|_{\varepsilon} &\leq (1+\varepsilon)\sum_{m=1}^{l}\left(-a_{m,l+1}^{(\alpha)}\right)C\Lambda\,(1+\varepsilon)^{l-m}\,p_{l-m-1}^{-1}\left((\Delta t)^{2-\alpha}+(\Delta x)^{2}\right)\\ &+ (1+\varepsilon)\,C\Lambda\left((\Delta t)^{2-\alpha}+(\Delta x)^{2}\right)\\ &\leq C\left((\Delta t)^{2-\alpha}+(\Delta x)^{2}\right)(1+\varepsilon)^{l+1}\,p_l^{-1}\left(\sum_{m=1}^{l}\left(-a_{m,l+1}^{(\alpha)}\right)+p_l\right) \qquad (4.17)\end{aligned}$$

Since

$$\sum_{m=1}^{l}\left(-a_{m,l+1}^{(\alpha)}\right)+p_l=(p_0-p_1+p_1-p_2+...+p_{l-1}-p_l)+p_l=p_0=1,$$

from (4.17) it follows

$$\left\|\mathbf{e}^{l+1}\right\|_{\varepsilon}\leq C\left((\Delta t)^{2-\alpha}+(\Delta x)^{2}\right)(1+\varepsilon)^{l+1}\,p_l^{-1},$$

and by induction (4.13) is valid for $l\in\mathbb{N}$.

THEOREM **4.2**. *Let $0<\varepsilon\leq\Delta t$, if the solution of (2.1) is of class C^2 with respect to t and of class C^4 with respect to x, then there exists a constant C_0 independent of Δx and Δt such that,*

$$\left\|\mathbf{e}^{l}\right\|_{\varepsilon}\leq C_0\left((\Delta t)^{2-\alpha}+(\Delta x)^{2}\right),\quad l=0,1,\ldots. \qquad (4.18)$$

P r o o f. From (4.13), the $\left\|\mathbf{e}^{l}\right\|_{\varepsilon}$ satisfies

$$\begin{aligned}\left\|\mathbf{e}^{l}\right\|_{\varepsilon} &\leq \frac{l^{-\alpha}}{p_l}C\Gamma(2-\alpha)l^{\alpha}\,(\Delta t)^{\alpha}\,(1+\varepsilon)^{l}\left((\Delta t)^{2-\alpha}+(\Delta x)^{2}\right)\\ &\leq \frac{l^{-\alpha}}{p_l}C\Gamma(2-\alpha)\,T^{*\alpha}\,(1+\varepsilon)^{l}\left((\Delta t)^{2-\alpha}\,(\Delta x)^{2}\right),\quad l=0,1,\ldots.\end{aligned}$$

On the other hand,

$$\begin{aligned}\lim_{l\to\infty}\frac{l^{-\alpha}}{p_l} &= \lim_{l\to\infty}\frac{l^{-\alpha}}{(l+1)^{-\alpha}-l^{-\alpha}}\\ &= \frac{1}{1-\alpha}\lim_{l\to\infty}\left(1-\frac{1}{l}\right)^{\alpha}=\frac{T^{*\alpha}}{1-\alpha}. \qquad (4.19)\end{aligned}$$

Thus, for $0<\varepsilon\leq\triangle t$, $(1+\varepsilon)^{n+1}\leq e^{T^*}$ it follows (4.18), for some positive constant C_0 that does not depend on Δt and Δx. □

Note that the convergence order depends on the fractional order α. For a method presenting optimal order convergence without the need to impose inconveniente smoothness conditions on the solution, see the work by Ford et al. [12].

5. Methodology Assessment

In order to illustrate the effectiveness of the method, some examples for which the analytical solution is known are presented. The error is measured by determining the maximum error at the mesh points (x_i, t_l):

$$\varepsilon_{\Delta x,\Delta t} = \max_{i=1,\ldots,N,\, l=0,\ldots,R} \left| T(x_i,t_j) - T_i^l \right|, \tag{5.1}$$

where T_i^l is the numerical solution at (x_i, t_l).

Example **5.1**.

$$\begin{cases} \dfrac{\partial^\alpha T(x,t)}{\partial t^\alpha} &= \dfrac{\partial}{\partial x}\left((x+1)\dfrac{\partial T(x,t)}{\partial x}\right) + t^{3/2}x^2\left(\dfrac{3}{2}-x\right) \\ & \quad -T(x,t) - 3t^{3/2}\left(1-3x^2\right) - \dfrac{3\sqrt{\pi}t^{3/2-\alpha}x^2\left(2x-3\right)}{8\Gamma\left(\frac{5}{2}-\alpha\right)} \\ T(x,0) &= 0, \;\; x \in (0,1) \\ \left.\dfrac{\partial T(x,t)}{\partial x}\right|_{x=0,1} &= 0, \;\; t \in (0,1) \end{cases} \tag{5.2}$$

whose analytical solution is $T(x,t) = t^{3/2}x^2\left(\frac{3}{2}-x\right)$, and,

Example **5.2**.

$$\begin{cases} \dfrac{\partial^\alpha T(x,t)}{\partial t^\alpha} = \dfrac{\partial}{\partial x}\left((x+1)\dfrac{\partial T(x,t)}{\partial x}\right) - \cos(t)\, t^2\left(x-\dfrac{x^4}{4}\right) - t^2\left(-1+3x^2+4x^3\right)\cos(t) \\ \qquad -\dfrac{(-4+x^3)xt^{-\alpha}}{4}\left(\dfrac{2t^2\,{}_2F_3\left(\left\{1,\frac{3}{2}\right\},\left\{\frac{1}{2};\frac{3}{2}-\frac{\alpha}{2},2-\frac{\alpha}{2}\right\};-\dfrac{t^2}{4}\right)}{\Gamma(3-\alpha)}\right) \\ \qquad +\dfrac{(-4+x^3)xt^{-\alpha}}{4}\left(\dfrac{6t^4\,{}_2F_3\left(\left\{2,\frac{5}{2}\right\},\left\{\frac{3}{2};\frac{5}{2}-\frac{\alpha}{2},3-\frac{\alpha}{2}\right\};-\dfrac{t^2}{4}\right)}{\Gamma(5-\alpha)}\right) - T(x,t)) \\ T(x,0) = 0, \;\; x\in(0,1) \\ \left.\dfrac{\partial T(x,t)}{\partial x}\right|_{x=0} = t^2\cos(t), \;\; \left.\dfrac{\partial T(x,t)}{\partial x}\right|_{x=1} = 0, \quad t\in(0,1) \end{cases} \tag{5.3}$$

whose analytical solution is $T(x,t)=\cos(t)\,t^2\left(x-\frac{x^4}{4}\right)$, with ${}_2F_3\left(...;...;...\right)$ the generalised hypergeometric function.

In Tables 1 and 2, we show the time and space convergence orders obtained for Ex. **5.1** using two different values of α ($\frac{1}{2}$ and $\frac{3}{4}$). Note that the analytical solution is not smooth at $t=0$, and therefore, we are expecting a reduction on the theoretical convergence order (the convergence order depends on α $\left(O\left((\triangle t)^{2-\alpha}\right)\right)$, and so, for a smooth function, we would obtain in the limit of a highly refined mesh, an experimental convergence order of 1.5 when $\alpha=0.5$ and 1.25 when $\alpha=0.75$).

For the space variable, we obtain an experimental convergence order of 2 (in the limit of a highly refined mesh), while for time, the convergence order slightly decreased, as expected, being 1.35 for $\alpha=0.5$ and 1.22 for $\alpha=0.75$. Nevertheless, the computations were easily performed, indicating that the method can deal with nonsmooth solutions.

Ex. **5.2** was also used to test the convergence order of the method. In this case, the imposed temperature flux is a sinusoidal function of time, that may be interpreted physically as a pulsating temperature applied at the surface of an object. In this case, the analytical solution is a smooth function in both time and space.

The results presented in Tables 3 and 4, show that the convergence orders obtained, match the theoretical predictions, reinforcing the robustness of the numerical method proposed. Fig. 3 shows the pronounced effect of the sinusoidal boundary condition, resulting in a wavy variation of $T(x,t)$ with t for $x=0.75$. A perfect match is found between the analytical and the numerical results, for $\triangle x=0.05$ and $\triangle t=0.05$.

TABLE 1. Numerical results obtained for the problem given in Eq. 5.2, for two different values of α ($\frac{1}{2}$ and $\frac{3}{4}$) : values of the maximum of the absolute errors at the mesh points and the experimental orders of convergence p, for the variable t ($\Delta x = 0.002$).

Step-sizes		$\alpha = 3/4$		$\alpha = 1/2$	
Δt	Δx	$\varepsilon_{\Delta x,\Delta t}$	p	$\varepsilon_{\Delta x,\Delta t}$	p
1/16	0.002	0.00207	–	0.00185	–
1/32	0.002	0.00090	1.19	0.00075	1.33
1/64	0.002	0.00039	1.21	0.00030	1.35
1/128	0.002	0.00017	1.22	0.00012	1.35

TABLE 2. Numerical results obtained for the problem given in Eq. 5.2, for two different values of α ($\frac{1}{2}$ and $\frac{3}{4}$) : values of the maximum of the absolute errors at the mesh points and the experimental orders of convergence q, for the variable x ($\Delta t = 0.001$).

Step sizes		$\alpha = 3/4$		$\alpha = 1/2$	
Δt	Δx	$\varepsilon_{\Delta x,\Delta t}$	q	$\varepsilon_{\Delta x,\Delta t}$	q
0.001	1/8	0.02687	–	0.02929	–
0.001	1/16	0.00718	1.91	0.00780	1.91
0.001	1/32	0.00183	1.97	0.00201	1.96
0.001	1/64	0.00045	2.04	0.00051	1.99

TABLE 3. Numerical results obtained for the problem given in Eq. 5.3, for $\alpha = 0.9$: values of the maximum of the absolute errors at the mesh points and the experimental orders of convergence p, for the variable t ($\Delta x = 0.002$).

Step-sizes		$\alpha = 0.9$	
Δt	Δx	$\varepsilon_{\Delta x,\Delta t}$	p
1/10	0.002	0.00929	–
1/20	0.002	0.00449	1.05
1/40	0.002	0.00213	1.08
1/80	0.002	0.00100	1.09

Note that the numerical method was derived for the numerical solution of equations that are simpler than the ones presented in the two previous examples. Nevertheless, the numerical method proved to be robust, providing the theoretical results we were expecting. The reason for choosing these two examples, was based on the lack of analytical solutions for fractional differential equations with the structure of equation (2.1).

TABLE 4. Numerical results obtained for the problem given in Eq. 5.3, for $\alpha = 0.9$: values of the maximum of the absolute errors at the mesh points and the experimental orders of convergence p, for the variable x ($\Delta t = 0.001$).

Step sizes		$\alpha = 0.9$	
Δt	Δx	$\varepsilon_{\Delta x,\Delta t}$	q
0.001	1/4	0.06052	–
0.001	1/8	0.01855	1.71
0.001	1/16	0.00513	1.85
0.001	1/32	0.00038	1.90

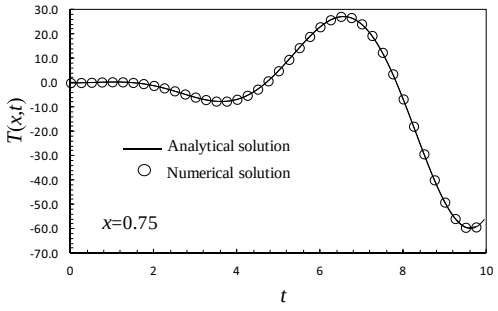

FIGURE 3. Variation of $T(x,t)$ with t for a constant $x = 0.75$.

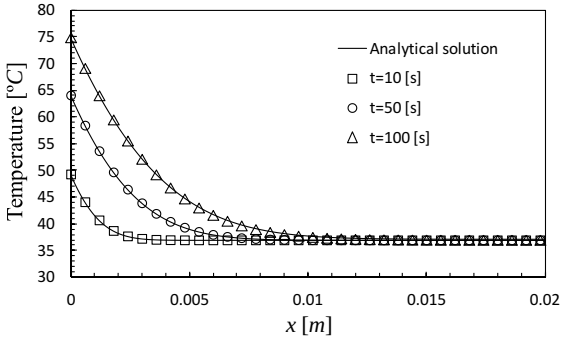

FIGURE 4. Variation of temperature along the space for three different times. Comparison between the numerical and analytical results.

For validation purposes, we also compared the results obtained by our method with the analytical solution (5.4) derived by [36] for the classical

Bioheat equation (1.1).

$$T(x,t) = T_a + \frac{q_0}{\sqrt{4kW_bc_b}} \left[\begin{array}{l} e^{-\sqrt{\frac{W_bc_b}{k}}x} erfc\left(\frac{x}{\sqrt{\frac{4kt}{c_t\rho_t}}} - \sqrt{\frac{W_bc_b}{c_t\rho_t}t} \right) \\ -e^{\sqrt{\frac{W_bc_b}{k}}x} erfc\left(\frac{x}{\sqrt{\frac{4kt}{c_t\rho_t}}} + \sqrt{\frac{W_bc_b}{c_t\rho_t}t} \right) \end{array} \right] \quad (5.4)$$

For this particular case, the case study was the temperature response of a semi-infinite biological tissue. Therefore, we chose the same coefficients as the ones given in [6], but, we set the metabolic heat generation to zero. We have used $\rho_t = 1050\,[kg/m^3]$, $c_t = 4180\,[J/\,(kg\,^\circ C)]$, $k = 0.5\,[J/(s.m\,^\circ C)]$, $W_b = 0.5\,[kg/\,(s.m^3)]$, $c_b = 3770\,[J/\,(kg\,^\circ C)]$, $T_a = 37^\circ C$, $L = 0.02m$, $q_0 = 5000$ and $q_m = 0\,[J/(s.m^3)]$.

Fig. 4 shows the variation of temperature, T, with time, t, for a constant value of x. The results were obtained for $\triangle x = 0.0001$ and $\triangle t = 0.25$, for three different time intervals. Since the analytical solution was derived for $\alpha = 1$ [36], we used a value of α closer to 1 ($\alpha = 0.999$). As shown, a good agreement was obtained between the numerical and the analytical solutions. We can also see that the temperature increases with time, due to the influence of the source term that represents the perfusion of blood.

6. Case Study

In order to test the influence of the time-fractional derivative on the classical bioheat equation, we used as a case study, the heating of skin assuming we have a geometry as the one shown in Fig. 5, where different layers of skin are shown. For this problem, three different case studies were considered: (I) the tissue is only formed by one layer; (II) three layers are considered, the epidermis, dermis, and, the subcutaneous tissue, with the space variable, x, ranging from 0 to 0.005 $[m]$; (III) the parameter τ is used to fit the experimental data. For the second case study, since the thermal conductivities of the epidermis, dermis and subcutaneous tissue, are given by 0.23, 0.45 and 0.19 $[W/(m\,^\circ C)]$, respectively, we will use a logistic function to perform the smooth passage between the different layers of skin, allowing this way to test the robustness of the numerical method.

Case study 1: For ease of understanding, the first numerical tests were performed assuming a constant thermal conductivity, k. For that purpose we used the epidermis tissue properties $\rho_t = 1200$, $c_t = 3590$, $k = 0.23$, although other properties could have been used, since the aim of this first case is to illustrate the general influence of the time-fractional derivative on the temperature distribution. For demonstration purposes we have also considered a blood perfusion rate of $W_b = 0.5$ [6], a specific heat of $c_b = 3770$,

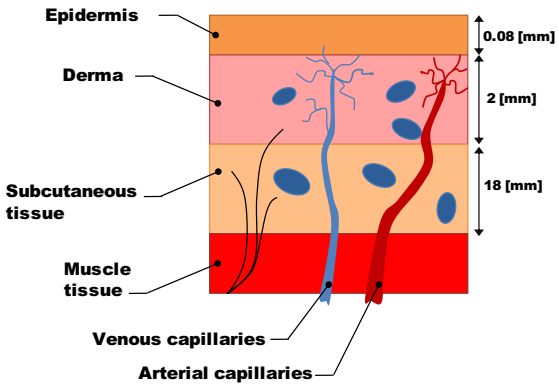

FIGURE 5. Different skin layers.

and an arterial blood temperature of $T_a = 37$ (note that the epidermis perfusion rate is zero [17]). The length of the epidermis is approximately $0.08\,[mm]$, but, for this case study we considered a larger tissue portion ($L = 0.02\,[m]$) so that the zero gradient boundary condition is not affecting the overall temperature distribution. Addtionally, the metabolic heat generation q_m and the temperature flux q_0 on the skin surface are assumed to be, respectively, 0 and 5000 $\left[J/(s.m^3)\right]$.

As remarked previously, in the literature we can find studies that make use of the time-fractional derivative, not taking into account the fact that the substitution of the classical time derivative by its generalised version, results in a change of units. The results obtained with such dimensionally inconsistent equation are equivalent to the ones obtained with the model proposed in this work, assuming $\tau = 1$. Therefore, Fig. 6 shows the variation of temperature along time, using different values for τ. In Fig. 6 (a) we consider $\tau = 1$ (being mathematically equivalent to equation (1.2)), and, in Figs. 6 (b), (c) and (d) we test the influence of τ on the temperature diffusion along the tissue and time.

As expected, the temperature increases with time (due to the perfusion of blood). Also, initially the temperature increases with α, and, the opposite behavior occurs after a certain period (Fig. 6 (a)). A similar behaviour was observed by Murio [29].

Figs. 6 (b) and (c) show that for the range of values studied, the parameter τ has a small influence on the temperature variation. This was expected, since the change in τ can be seen as a small change in the density and specific heat. The influence of τ on the temperature variation is expected to increase for smaller values of α, as shown in Fig. 6 (d). In these problems, the mesh used was $\triangle x = 0.0001$ and $\triangle t = 0.01$.

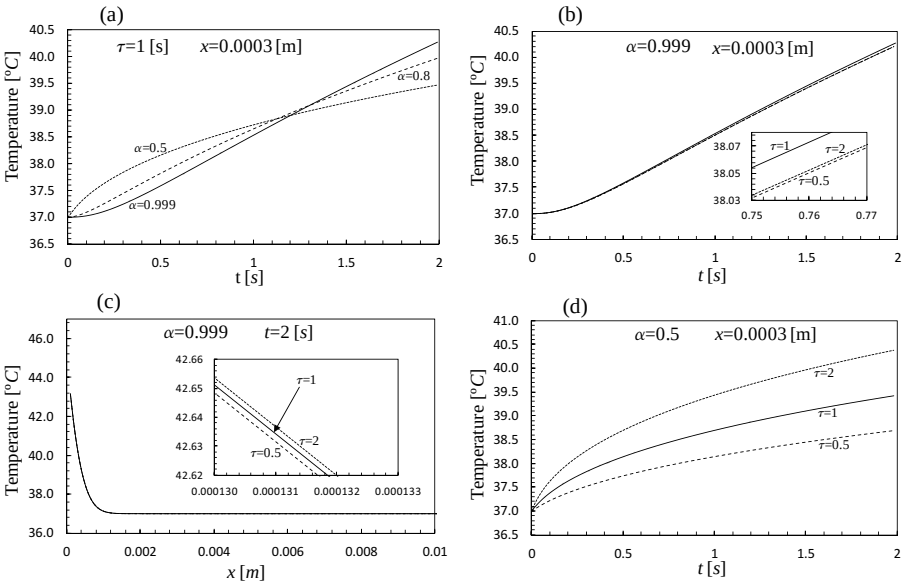

FIGURE 6. Variation of temperature along time ($x = 0.0003\,[m]$) and space ($t = 2\,[s]$). (a) $\tau = 1$ and three different values of α. (b) and (c)$\alpha = 0.999$ and three different values of τ. (d) $\alpha = 0.5$ and three different values of τ.

Case study 2: For the second case we have taken into account three different layers of skin, the epidermis, the dermis and the subcutaneous tissue. The density and the specific heat are the ones from the subcutaneous region, that is, $\rho_t = 1000$, $c_t = 2675$. The thermal conductivity function is given by $k\,(x) = 0.23 + (1 + \exp\,[m\,(-x + 0.00008)])^{-1}\,0.45 - (1 + \exp\,[m\,(-x + 0.00208)])^{-1}\,0.26$, and $L = 0.005\,[m]$ (with m a parameter that allows tuning the variation of k between two layers. For this particular case we have considered $m = 100000$). The perfusion rate and blood properties are the ones presented before, and, the metabolic heat generation is assumed to be $q_m = 368.1$.

Fig. 7 shows the variation of temperature along the different layers of skin, for $t = 2\,[s]$, and considering two different values of α (0.999 and 0.8).

Case study 3: In this last case study, we used the experimental data provided by Barcroft and Edholme [2] for the temperature variation inside a human arm. One of their experiments consisted of measuring the temperature decrease of the subcutaneous tissue ($1\,cm$ below the skin surface) when the forearm is submersed in a $12°C$ water bath (see Fig. 8 (a)). For the numerical tests we have assumed a 1D problem, and, even then, good

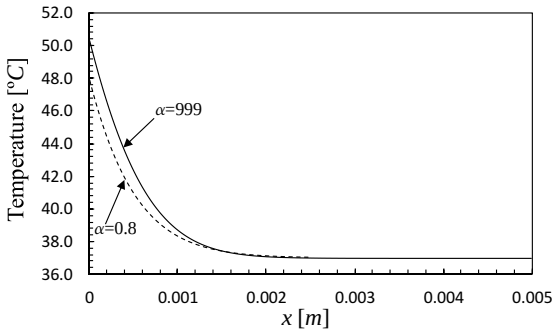

FIGURE 7. Variation of temperature for constant $t = 2\,[s]$ and two different values of α, 0.999 and0.8 ($\tau = 1$).

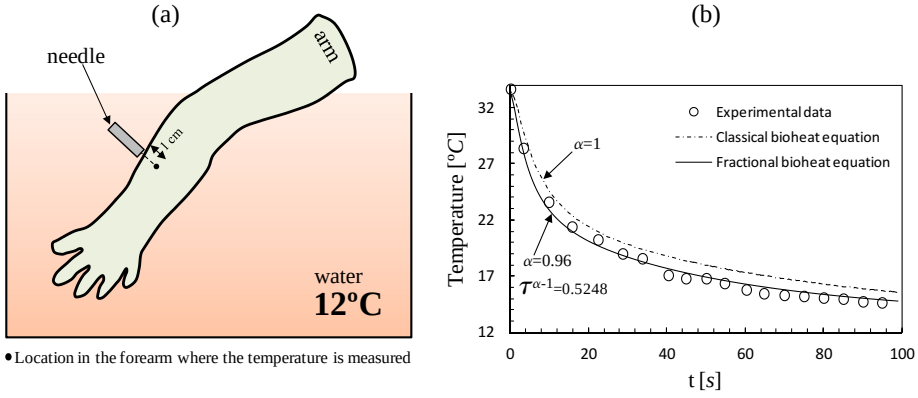

FIGURE 8. (a) Experimental setup. (b) Fitting experimental data (case study 3).

results were obtained by setting $\alpha = 0.96$ and and $\tau^{\alpha-1} = 0.5248$ (based on the data provided in the papers [2] and [40] we have used the following parameters: initial temperature of $33.6C$, $\rho_t = c_t = 1\,g/cm^3$, $\rho_b = c_b = 1\,[cal.g^{-1}.C^{-1}]$, $q_m = 0.0001\,[cal.s^{-1}.cm^{-3}]$, $k = 0.0015\,cal.s^{-1}.cm^{-1}.C^{-1}$, $W_b c_b = 0.000016$). The boundary conditions are given by,

$$\left.\frac{\partial T(x,t)}{\partial x}\right|_{x=0} = 0, \tag{6.1}$$

$$\left.-k\,\frac{\partial T(x,t)}{\partial x}\right|_{x=4\,[cm]} = 0.0075\,(T-12)\,. \tag{6.2}$$

In Fig. 8 (b), we show that the proposed fractional bioheat equation can be used to improve the accuracy of the numerical predictions.

7. Conclusions

In this work we proposed a generalisation of the classical bioheat equation, through the substitution of the rate of change term by a fractional time derivative. A numerical method was also devised to solve the proposed equation, which was proved to be stable and convergent. The numerical method proposed is general, and, can be used in the solution of other fractional diffusion equations.

We observed that with this fractional bioheat model, for a fixed x, and varying t from zero to a certain point $t_\alpha \sim 1$, when the order of the time derivative increases, the temperature decreases, and, after that point t_α, the opposite behavior is observed. The new model proved to be robust and more flexible than the classical bioheat equation, since it allowed us to obtain a better fit of experimental data.

Acknowledgements

The authors L.L. Ferrás and J. M. Nóbrega acknowledge financial funding by FEDER through the COMPETE 2020 Programme and by FCT - Portuguese Foundation for Science and Technology under the projects UID/CTM/50025/2013 and EXPL/CTM-POL/1299/2013. L.L. Ferrás acknowledges financial funding by the Portuguese Foundation for Science and Technology through the scholarship SFRH/BPD/100353/2014. M. Rebelo acknowledges financial funding by the Portuguese Foundation for Science and Technology through the project UID/MAT/00297/2013.

References

[1] S.I. Alekseev, M.C. Ziskin, Influence of blood flowand millimeter wave exposure on skin temperature in different thermal models. *Bioelectromagnetics* **30**, (2009), 52-58.

[2] H. Barcroft, O.G. Edholm, Temperature and blood flow in the Human forearm. *J. Physiol.* **104** (1946) 366-376.

[3] C. Cattaneo, Sulla Conduzione del Calore. *Atti Sem. Mat. Fis. Univ. Modena* **3**, (1948), 83101.

[4] C. Cattaneo, Sur une Forme de lquation de la Chaleur liminant le Paradoxe dune Propagation Instantane. *C. R. Acad. Sci.* **247**, (1958), 431-433.

[5] M.M. Chen. K.R. Holmes, Microvascular Contributions in Tissue Heat Transfer. *Ann. N. Y. Acad. Sci.* **335**, (1980), 137-150.

[6] R.S. Damor, S. Kumar , A.K. Shukla, Numerical solution of Fractional Bioheat Equation with Constant and Sinusoidal Heat flux coindition on skin tissue. *American Journal of Mathematical Analysis* **1**, (2013), 20-24.

[7] K. Diethelm, *The analysis of fractional differential equations: An application-oriented exposition using differential operators of Caputo type*, Springer (2010).

[8] C.R. Davies, G.M. Saidel, H. Harasaki, Sensitivity analysis of one-dimensional heat transfer in tissue with temperature-dependent perfusion. *J. Biomech. Eng.* **119**, (1997), 77-80.

[9] B. Erdmann, J. Lang, M. Seebass, Optimization of temperature distributions for regional hyperthermia based on a nonlinear heat transfer model. *Ann. N. Y. Acad. Sci.* **858**, (1998), 36-46.

[10] M.A. Ezzat, N.S. AlSowayan, Z.I.A. Al-Muhiameed, S.M. Ezzat, Fractional modelling of Pennes' bioheat transfer equation. *Heat Mass Transfer* **50**, (2014), 907-914; DOI: 10.1007/s00231-014-1300-x.

[11] N.J. Ford, M.L. Morgado, M. Rebelo, A numerical method for the distributed order time-fractional diffusion equation. In:*IEEE Explore Conference Proceedings, ICFDA'14 International Conference on Fractional Differentiation and Its Applications*, Catania, Italy (2014).

[12] N.J. Ford, M.L. Morgado, M. Rebelo, Nonpolynomial collocation approximation of solutions to fractional differential equations. *Fract. Calc. Appl. Anal.* **16**, (2013), 874-891.

[13] A.P. Gagge, Rational temperature indices of man's thermal environment and their use with a 2-node model of his temperature regulation. *Fed. Proc.* **32**, (1973), 1572-1582.

[14] A.P. Gagge, A.P. Fobelets, L.G. Berglund, A standard predictive index of human response to the thermal environment. *ASHRAE Trans.* **92**, (1986), 709-731.

[15] C. Gong, W. Bao, G. Tang, A parallel algorithm for the Riesz fractional reaction-diffusion equation with explicit finite difference method. *Fract. Calc. Appl. Anal.* **16**, (2013), 654-669.

[16] R. Gorenflo, F. Mainardi, D. Moretti, and P. Paradisi, Time Fractional Diffusion: A Discrete Random Walk Approach. *Nonlinear Dynamics* **29**, (2002), 129-143.

[17] T.R. Gowrishankar, D.A. Stewart, G.T. Martin, J.C. Weaver, Transport lattice models of heat transport in skin with spatially heterogeneous, temperature-dependent perfusion. *Biomed. Eng. Online* **3**, (2004), 42.

[18] M. E. Gurtin and A. C. Pipkin, A General Theory of Heat Conduction with Finite Wave Speeds. *Arch. Rational Mech. Anal.* **31**, (1968), 113-126.

[19] J.F. Huang, Y.F. Tang, W.J. Wang, J.Y. Yang, A compact difference scheme for time fractional diffusion equation with Neumann boundary conditions. In: *AsiaSim 2012, Asia Simulation Conference 2012, Part I*, Shanghai, China (2012), 273-284. doi: 10.1007/978-3-642-34384-1_33

[20] X. Jiang, H. Qi, Thermal wave model of bioheat transfer with modified Riemann–Liouville fractional derivative. *J. Phys. A: Math. Theor.* **45**, (2012), 485101 (11pp).

[21] W. Kaminski, Hyperbolic Heat Conduction Equation for Materials With a Nonhomogeneous Inner Structure. *J. Heat Transfer* **112**, (1990), 555-560.

[22] I. Karatay, N. Kale, S.R. Bayramoglu, A new difference scheme for time fractional heat equations based on the Crank-Nicholson method. *Fract. Calc. Appl. Anal.* **16**, (2013), 892-910.

[23] H.G. Klinger, Heat transfer in perfused biological tissue. I. General theory. *B. Math. Biol.* **36**, (1974), 403-415.

[24] A. Lakhssassi, E. Kengne, H. Semmaoui, Investigation of nonlinear temperature distribution in biological tissues by using bioheat transfer equation of Pennes' type. *Natural Science* **3**, (2010), 131-138.

[25] A. Lakhssassi, E. Kengne, H. Semmaoui, Modifed pennes' equation modelling bio-heat transfer in living tissues: analytical and numerical analysis. *Natural Science* **2**, (2010), 1375-1385.

[26] B. Li, J. Wang, Anomalous Heat Conduction and Anomalous Diffusion in One-Dimensional Systems. *Physical Review Letters* **91**, (2003), 044301- 1-4; DOI: http://dx.doi.org/10.1103/PhysRevLett.91.044301.

[27] W.J. Minkowycz, E.M. Sparrow, J.P. Abraham, *Advances in Numerical Heat Transfer: Volume 3*. CRC Press, Boca Raton, USA (2010).

[28] M. L. Morgado, M. Rebelo, Numerical approximation of distributed order nonlinear reaction-diffusion equations. *Journal of Computational and Applied Mathematics* **275**, (2015), 216-227.

[29] D.A. Murio, Implicit finite difference approximation for time fractional diffusion equations. *Computers & Mathematics with Applications* **56**, (2008), 1138-1145.

[30] J.-H. Niu, H.-Z. Wang, H.-X. Zhang, J.-Y. Yan, Y.-S. Zhu, Cellular neural network analysis for two dimensional bioheat transfer equation. *Med. Biol. Eng. Comput.* **39**, (2001), 601-604.

[31] W.L. Nyborg, Solutions of the bio-heat transfer equation. *Phys. Med. Biol.* **33**, (1988), 785-792.

[32] M.N. Özişik, D.Y. Tzou, On the Wave Theory in Heat Conduction. *J. Heat Transfer* **116**, (1994), 526-535.
[33] H.H. Pennes, Analysis of tissue and arterial temperatures in the resting human forearm. *J. Appl. Physiol.* **1**, (1948), 93-122.
[34] Y. Z. Povstenko, Fractional Heat Conduction Equation and Associated Thermal Stress. *J. Thermal Stresses* **28**, (2005), 83102.
[35] Y. Povstenko, Thermoelasticity Which Uses Fractional Heat Conduction Equation. *J. Math. Sci.* **162**, (2009), 296-305.
[36] T.-C. Shih, P. Yuan, W.-L. Lin, H.-S. Kou, Analytical analysis of the Pennes bioheat transfer equation with sinusoidal heat flux condition on skin surface. *Med. Eng. Phis.* **29**, (2007), 946-953.
[37] J. Sun, A. Zhang, L.X. Xu, Evaluation of alternate cooling and heating for tumor treatment. *International Journal of Heat and Mass Transfer* **51**, (2008), 5478-5485; doi:10.1016/j.ijheatmasstransfer.2008.04.027.
[38] M. Tunç, Ü. Çamdali, C. Parmaksizoğlu, S. Çikrikçi, The bioheat transfer equation and its applications in hyperthermia treatments. *Eng. Computation.* **23**, (2006), 451-463.
[39] S. Weinbaum, L.M. Jiji, D.E. Lemons, Theory and experiment for the effect of vascular microstructure on surface tissue heat transfer. Part I. Anatomical foundation and model conceptualization. *J. Biomech. Eng.-T. ASME* **106**, (1984), 321-330.
[40] E.H. Wissler, Pennes' 1948 paper revisited. *J. Appl. Physiol.* **85** (1998) 35-41.
[41] W. Wulff, The Energy Conservation Equation for Living Tissues. *IEEE Transactions- Biomedical Engineering* **21**, (1974), 494-495.
[42] A. Zolfaghari, M. Maerefat, A New Simplified Thermoregulatory Bioheat Model for Evaluating Thermal Response of the Human Body to Transient Environment. *Build. Environ.* **45**, (2010), 2068-2076.
[43] A. Zolfaghari,M. Maerefat, *Developments in Heat Transfer*, Edited by Marco Aurelio Dos Santos Bernardes, InTech (2011).

[1] *Institute for Polymers and Composites/I3N*
University of Minho
Campus de Azurém 4800-058 Guimarães, PORTUGAL
e-mail: luis.ferras@dep.uminho.pt
e-mail: mnobrega@dep.uminho.pt

Received: ...., 2015

[2] *Department of Mathematics*
University of Chester, CH1 4BJ, UK

e-mail: njford@chester.ac.uk

[3] *Department of Mathematics*
University of Trás-os-Montes e Alto Douro, UTAD
Quinta de Prados 5001-801, Vila Real, PORTUGAL
e-mail: luisam@utad.pt

[4] *Departamento de Matemática and Centro de Matemática e Aplicações*
Faculdade de Ciências e Tecnologia, Universidade Nova de Lisboa
Quinta da Torre, 2829-516 Caparica, PORTUGAL
e-mail: msjr@fct.unl.pt